ACS APPLIED MATERIALS & INTERFACES

www.acsami.org

Research Article

Water/Light Multiregulated Supramolecular Polypseudorotaxane Gel with Switchable Room-Temperature Phosphorescence

Songen Liu, Yi Zhang, Jianqiu Li, Conghui Wang, Yong Chen,* and Yu Liu*

Cite This: *ACS Appl. Mater. Interfaces* 2024, 16, 5149−5157

Read Online

ACCESS | Metrics & More | Article Recommendations | Supporting Information

ABSTRACT: Water/light regulated room-temperature phosphorescence (RTP) of polypseudorotaxane supramolecular gel is constructed by threading the poly(ethylene glycol)-*block*-poly(propylene glycol)-*block*-poly(ethylene glycol) (PEG−PPG-PEG) chain with the bromoaromatic aldehyde into mono-(6-ethylenediamine-6-deoxygenated)-*β*-cyclodextrin (ECD) cavities and further assembling with negatively charged Laponite XLG (CNS) and diarylethene derivative (DAE) through electrostatic interaction. This hydrogel exhibits significant blue fluorescence emission; instead, after lyophilization to xerogel, the system exhibits both blue fluorescence and yellow RTP based on the rigid network structure of the xerogel, which restricts the vibration of the phosphor and suppresses the nonradiative relaxation process. Interestingly, the addition of excess ECDs to the gel system can enhance the RTP emission. Furthermore, the reversible luminescence behavior can be adjusted by the photoresponsive isomerism of DAE and humidity. This polypseudorotaxane supramolecular gel system provides a novel strategy for constructing tunable RTP materials.

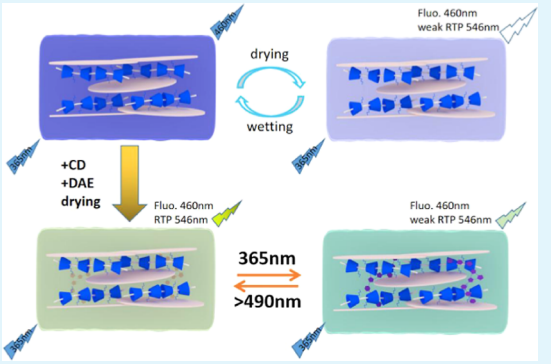

KEYWORDS: *supramolecular polypseudorotaxane, room-temperature phosphorescence, multistimulus response, cyclodextrin, multicolor materials*

INTRODUCTION

Recently, supramolecular systems with room-temperature phosphorescence (RTP) have been considered as more advantageous luminescent materials due to the distinctive properties, such as large Stokes shift and long triplet lifetime.[1−3] The macrocyclic confinement effect and the reversibility of supramolecular systems have attracted increasing research efforts to effectively enhance RTP through noncovalent interactions.[4−6] The encapsulation of macrocyclic hosts could restrict molecular motion of phosphorescent guests and even promote intersystem crossing (ISC) to enhance RTP emission.[7,8] In addition, the abundant hydrogen bonding interactions and ordered spatial structure of supramolecular assemblies supply a rigid microenvironment, which is able to stabilize the triplet state and inhibit nonradiative transitions to promote RTP.[9,10] For example, Xiao et al. constructed a new supramolecular hydrogel using 1,4-diaminobenzene (DB) and hexamethyl cucurbit[5]uril (HmeQ[5]) by the host−guest interaction, and then embedded 6-bromo-2-naphthol (BrNp) exhibited fluorescent−phosphorescence double emissions due to the rigid microstructure.[11] Multicolor luminescence,[12] especially multicolor RTP materials,[13] is a hot topic in the field of chemical materials. However, there are still some limitations in the regulation of the RTP emission. Therefore, tunable RTP materials responding to stimulus such as temperature,[14−16] humidity,[17−19] mechanical force,[20−22] pH,[23−25] and light[26−29] have attracted extensive attention, revealing their broad application prospects in chemical sensing,[30,31] information anticounterfeiting,[32,33] optoelectronic devices,[34,35] and biological imaging.[9,36]

As a novel functional material with fast swelling, high water content, and good biocompatibility, hydrogel shows great potential application value.[37] Therefore, it is increasingly necessary to develop supramolecular hydrogel materials with RTP emission.[38,39] The polypseudorotaxane can be formed by cyclodextrin (CD) threading the polymer chain,[40] which is able to be used as the dominant building block of luminescent supramolecular hydrogels by utilizing the reversible encapsulation of CDs with polymer chains to achieve stimulus response. Herein, polypseudorotaxane shows an efficient strategy for constructing stimulus-responsive supramolecular RTP hydrogels.[41] Yang et al. reported luminescent dimers (6-NDI-CDs) prepared by bridging different cyclodextrins with 1,4,5,8-naphthalimide (NDI). Polyacrylamide introduced by tetraammonium axle copolymers could assemble with 6-NDI-

Received: November 16, 2023
Revised: December 25, 2023
Accepted: January 11, 2024
Published: January 22, 2024

https://doi.org/10.1021/acsami.3c17214
ACS Appl. Mater. Interfaces 2024, 16, 5149−5157

Scheme 1. Schematic Illustration of the Building of Multistimulus Response Supramolecular Gel

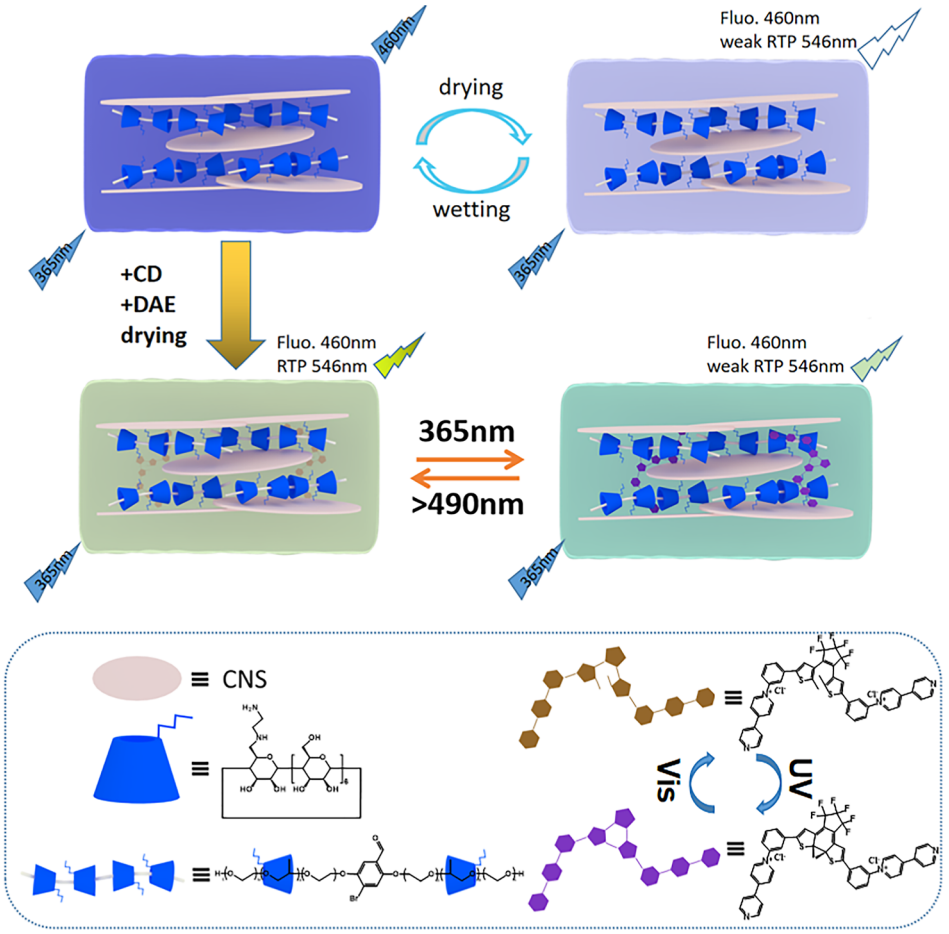

CDs and cucurbit[6]uril (CB [6]) to construct the supramolecular hydrogel, which showed excellent ductility and unique photoinduced color change characteristics, and was able to erase discoloration by stretching the hydrogel.[42] Liu et al. reported a photocontrolled reversible multicolor RTP emission supramolecular polypseudorotaxane system constructed from CD and polyethylene glycol (PEG) derivatives modified with benzene and naphthalene as luminophores. The RTP of the system could be reversibly regulated through the photoisomerization of DAE.[43] Moreover, the polymer formed by the bromoaromatic aldehyde and PEG could emit blue fluorescence in the presence of water and both blue fluorescence and yellow RTP after drying, thus realizing the drying−wetting luminescence regulation of gel.[44] Different from the previously reported single stimuli response phosphorescence regulation system, we constructed a triple stimulus response supramolecular gel system that could be regulated by macrocyclic, water, and light. Herein, a bromoaromatic aldehyde block polymer (PEG−PPG-PEG) chain that could thread the ethylenediamine-β-cyclodextrins to form polypseudorotaxane was prepared. Polypseudorotaxane and CNS were assembled through electrostatic interactions to obtain supramolecular hydrogels with blue fluorescence. The addition of CNS enhanced the mechanical properties of the hydrogel system, especially its self-healing ability. After freeze-drying, the dry xerogel showed a weak yellow RTP emission. Importantly, the RTP emission colors of the supramolecular xerogel changed when different proportions of ECDs were added. Moreover, DAE was added as optical switches to control the RTP emission of the system under light stimulation (Scheme 1). Therefore, due to reversible multistimulus response, this gel system is convenient to be applied in the multicolor luminescence.

RESULTS AND DISCUSSION

The polypseudorotaxane hydrogel system could be constructed conveniently as follows: the polymer **G** with the bromoaromatic aldehyde as the core and PEG−PPG-PEG (PEG: PPG = 1:9) as the side chain was synthesized in 52.3% yield, where PPG units could well associate with the β-CD cavity. Therefore, ECDs could form polypseudorotaxane with polymer **G** in aqueous solution. 2D ROESY spectra exhibited the significant correlation between the inner protons of ECD cavities and the methyl protons of the PPG unit of **G**, indicating that ECD cavities were threaded on the polymer chain to form a polypseudorotaxane (Figure S11). Through a calculation based on the ^{1}H NMR spectrum, each polypseudorotaxane contained 13.3 ECDs (Figure S12).[45] Then, hydrogel **1** could be prepared by electrostatic interactions between pseudorotaxane and negatively charged CNS (Figure S13; **1**, the mass ratio of pseudorotaxane: ECD was 1:0). CNS is a kind of inorganic nanosheet with negative charges on the surface, which can combine with pseudorotaxane to form a stable three-dimensional hydrogel network through electrostatic interaction. Therefore, hydrogels have good mechanical strength and exhibit excellent self-healing properties. Zeta

https://doi.org/10.1021/acsami.3c17214
ACS Appl. Mater. Interfaces 2024, 16, 5149−5157

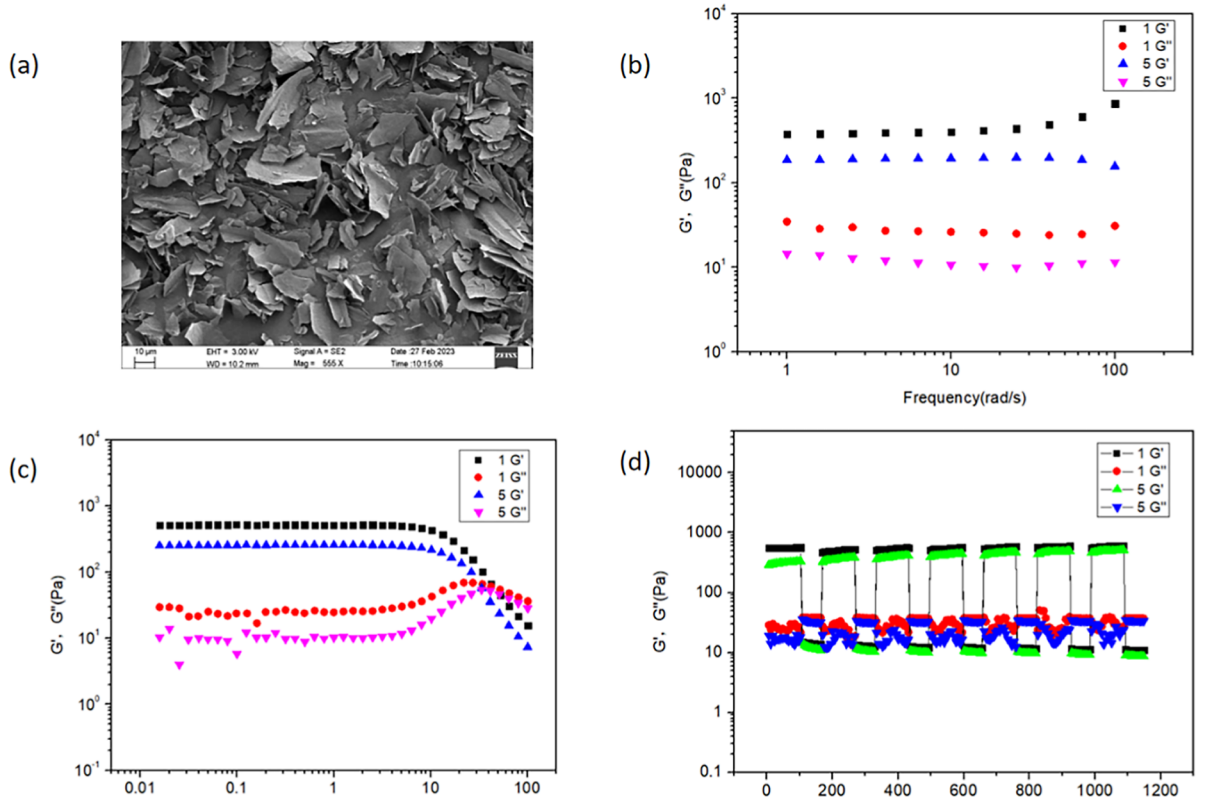

Figure 1. (a) SEM images of xerogel **1**. (b) Frequency sweep tests of the hydrogels **1** and **5** at ω = 0.01−100 rad s^{-1} and strain (γ) = 1% at 25 °C. (c) Strain sweep tests of the hydrogels **1** and **5** at γ = 0.01−100% with ω = 6.28 rad s^{-1}. (d) Continuous step strain tests of hydrogels **1** and **5** at γ = 0.05 and 100%.

potential measurements gave an average zeta potential of CNS aqueous solution as −42.69 mV and hydrogel **1** aqueous solution as −35.75 mV (Figure S14), indicating that the electrostatic interaction is favorable. After lyophilization, scanning electron microscopy (SEM) images (Figure 1a) indicated the morphology of xerogel **1** as lamellar nanosheets. Furthermore, a series of supramolecular hydrogels **2**−**5** with various pseudorotaxane/excess ECD ratios (the mass ratios of pseudorotaxane: ECD values of 1:0.06, 1:0.1, 1:0.5, and 1:1, respectively) were also constructed, exploring the changes of luminescence behavior under different ECD ratios.

Subsequently, we tested the rheological properties of supramolecular hydrogels to explore their mechanical properties. Taking hydrogels **1** and **5** as examples, the frequency sweep test was carried out under the condition of strain (γ) = 1%, and the curves of storage modulus (G') and loss modulus (G'') of hydrogels increased with the increase of oscillating strain (Figure 1b). Under 100 to 0.01% oscillating strain, G' was always greater than G'', implying that the hydrogel was always stable under strain γ = 1%, and the physical cross-linking remained unchanged. The amplitude sweep experiments exhibited the variation of G' and G'' as the oscillation strain increased (Figure 1c). At the angular frequency ω = 6.28 rad s^{-1}, hydrogels **1** and **5** underwent a transition of sol−gel state under the critical strain (γ = 20%), indicating that the hydrogel network was destroyed. When the change of strain γ was between 0.01% and 20%, G' was higher than G'', implying that supramolecular hydrogels were still not easily destroyed and had good stability. However, when strain γ was higher than 20%, G'' was higher than G', proving the destruction of hydrogel networks, and the system changed from gel to sol. Furthermore, continuous step strain tests exhibited the self-healing performance of hydrogels **1** and **5** (Figure 1d). When placed under high strain (γ = 100%, ω = 6.28 rad s^{-1}) for 100 s, the G' values of the system were significantly reduced, and the structure was destroyed. Instead, the values of G' and G'' returned rapidly to the initial state, and the system recovered to hydrogels when the strain decreased (γ = 0.05%, ω = 6.28 rad s^{-1}) for 60 s. It is worth noting that this reversible strain-responsive gel−sol phase transition demonstrated that supramolecular hydrogels possessed satisfactory self-healing properties.

A series of spectral experiments were conducted to investigate the luminescence behavior of the hydrogel system. Hydrogel **1** showed strong blue fluorescence at 460 nm but no RTP emission (Figure 2a). In addition, the Commission Internationale de l'ÉClair-age (CIE) coordinates of the fluorescence emission of hydrogel were calculated to be (0.18, 0.21) (Figure S15), accompanied by a lifetime of 8.94 ns (Figure S16). When the hydrogel was freeze-dried, the obtained xerogel **1** showed both blue fluorescence and yellow phosphorescence emission. Photoluminescence spectra of xerogel **1** under an excitation of 365 nm showed that xerogel **1** still had blue fluorescence emission (Figure 2b). However, time-resolved delayed photoluminescence spectra exhibited yellow RTP emission at 546 nm. The coordinates of the photoluminescence CIE chromaticity diagram of the xerogel were (0.23, 0.27), and the coordinates of the delayed photoluminescence CIE chromaticity diagram were (0.41, 0.53) (Figure S17). The fluorescence lifetime and the fluorescence quantum yield of xerogel were 9.52 ns and 6.66%, respectively, but the lifetime and quantum yield of

https://doi.org/10.1021/acsami.3c17214
ACS Appl. Mater. Interfaces 2024, 16, 5149−5157

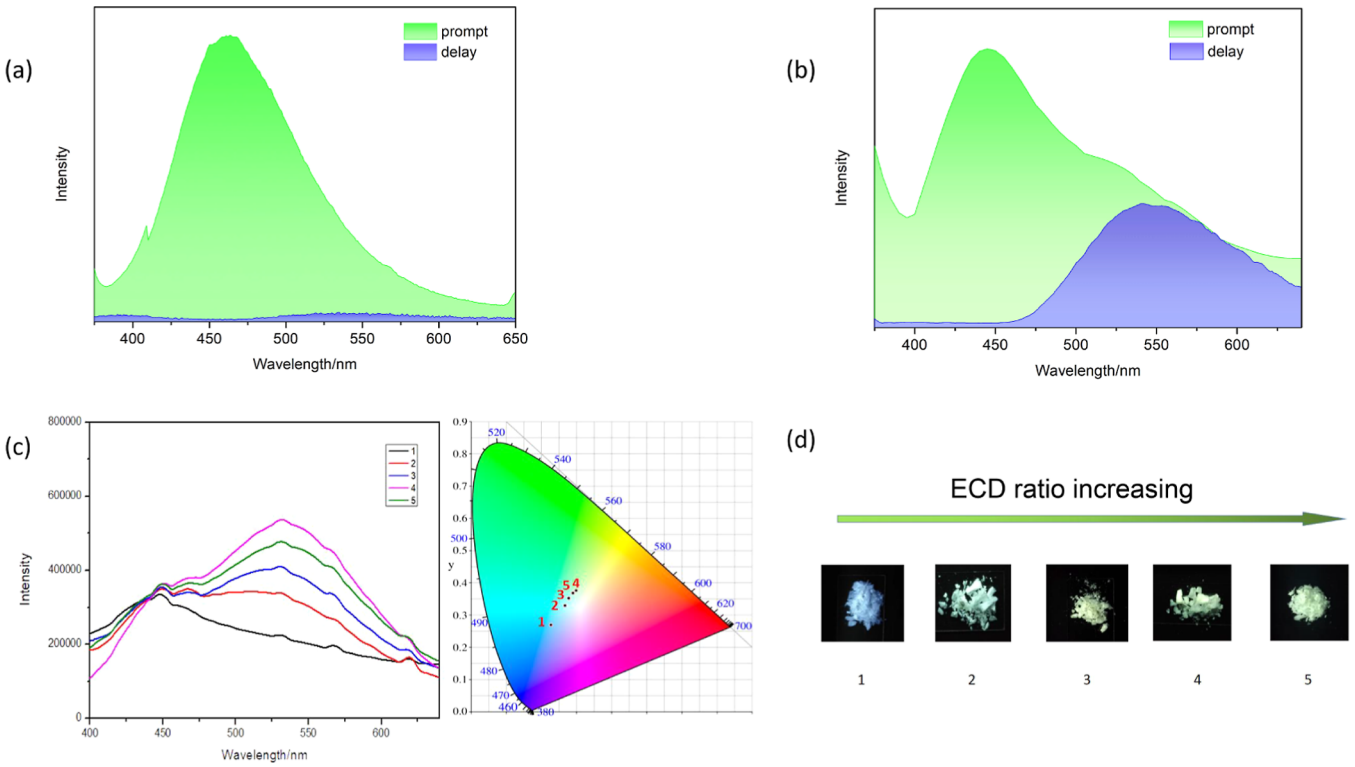

Figure 2. (a) Prompt photoluminescence spectra and delayed photoluminescence spectra of hydrogel **1** (delayed 50 μs; λ_{ex} = 365 nm). (b) Prompt photoluminescence spectra and delayed photoluminescence spectra of xerogel **1** (delayed 50 μs; λ_{ex} = 365 nm). (c) Photoluminescence emission spectrum and CIE chromaticity diagrams of xerogels **1**−**5** with different mass fractions of ECDs (**1**, pseudorotaxane/ECD = 16/0 wt %; **2**, pseudorotaxane/ECD = 16/0.96 wt %; **3**, pseudorotaxane/ECD = 16/1.6 wt %; **4**, pseudorotaxane/ECD = 15/7.5 wt %; **5**, pseudorotaxane/ECD = 14/14 wt %; λ_{ex} = 365 nm). (d) Photographs of xerogels **1**−**5** with different mass fractions of ECDs under UV light (λ_{ex} = 365 nm).

phosphorescence were 6.60 ms and 6.41%, respectively (Figures S19 and S20). The possible reason for the RTP emission of the gel system may be due to the following reasons: (1) the hydrophobic cavity of ECD on pseudorotaxane provided space relaxation restriction for **G**, which promoted phosphorescence emission; (2) the formation of the gel network structure provided a protective environment for effectively immobilizing **G** and inhibiting the nonradiative relaxation process leading to RTP emission; and (3) the rigid structure of xerogel was stable, which was capable of exhibiting a stronger RTP emission.[44,46]

Although the xerogel had fluorescence−phosphorescence double emission, the RTP emission intensity of xerogel **1** was still low. To enhance the RTP emission of this system, different proportions of ECDs were added to obtain gel systems **2**−**5**. As the amount of ECDs increased, the RTP emission intensities of the gel system increased sequentially, which was consistent with the coordinate position in the CIE chromaticity diagram of photoluminescence. It could be seen that five emission points were located in the same straight line, indicating that the RTP intensity continuously increased with the increase of ECDs, and the emission color changed continuously (Figure 2c; Table S1). Typically, xerogel **5** showed light-yellow luminescence under 365 nm UV light, accompanied by a fluorescence lifetime of 5.54 ns (fluorescence quantum yield: 4.48%) and a phosphorescence lifetime of 3.66 ms (phosphorescence quantum yield: 13.51%). The SEM image (Figure S24) of xerogel **5** showed a morphology as nanosheets. Similarly, we could regulate the luminescence color of the xerogel continuously changing from blue to yellow by adding different proportions of ECDs (Figure 2d).

Considering that the hydrogel only exhibited blue fluorescence at 460 nm, while xerogel had blue fluorescence emission at 460 nm and yellow phosphorescence emission at 546 nm under 365 nm UV light, we infer that the humidity had a significant impact on the RTP intensity of gel system, which is due to the fact that the content of water in the gel system could accelerate the nonradiative relaxation process and ultimately prompt a significant reduction in RTP emission. Hence, we used two different sets of samples **1** and **5** to investigate their luminescence behavior before and after moistening. Delayed photoluminescence spectra of xerogel **1** are shown in Figure 3a. Under drying conditions, **1** had a weak yellow RTP, but the RTP further weakened after moistening. Xerogel **5** had a strong RTP emission under drying conditions but decreased significantly after moistening (Figure 3b). The photoluminescence spectra of xerogels **1** and **5** before and after moistening by water also showed the change of luminescence of the gel system (Figure S25). Taking **5** as an example, the multicolored luminescence of the gel system could be reversibly repeated for at least 7 cycles by drying−wetting regulation (Figure 3c). Therefore, we investigated the reversible photoluminescence behavior of xerogels **1** and **5** under drying−wetting switch conversion conditions. As shown in Figure 3a, solid state **1** exhibited light-blue luminescence. After the drop of water onto **1**, the emission color turned deep blue. After drying, **1** recovered light-blue luminescence. Similarly, the solid state **5** exhibited a light-yellow luminescence but turned greenish-blue by moistening, and then recovered light yellow after drying (Figure 3b).

https://doi.org/10.1021/acsami.3c17214
ACS Appl. Mater. Interfaces 2024, 16, 5149−5157

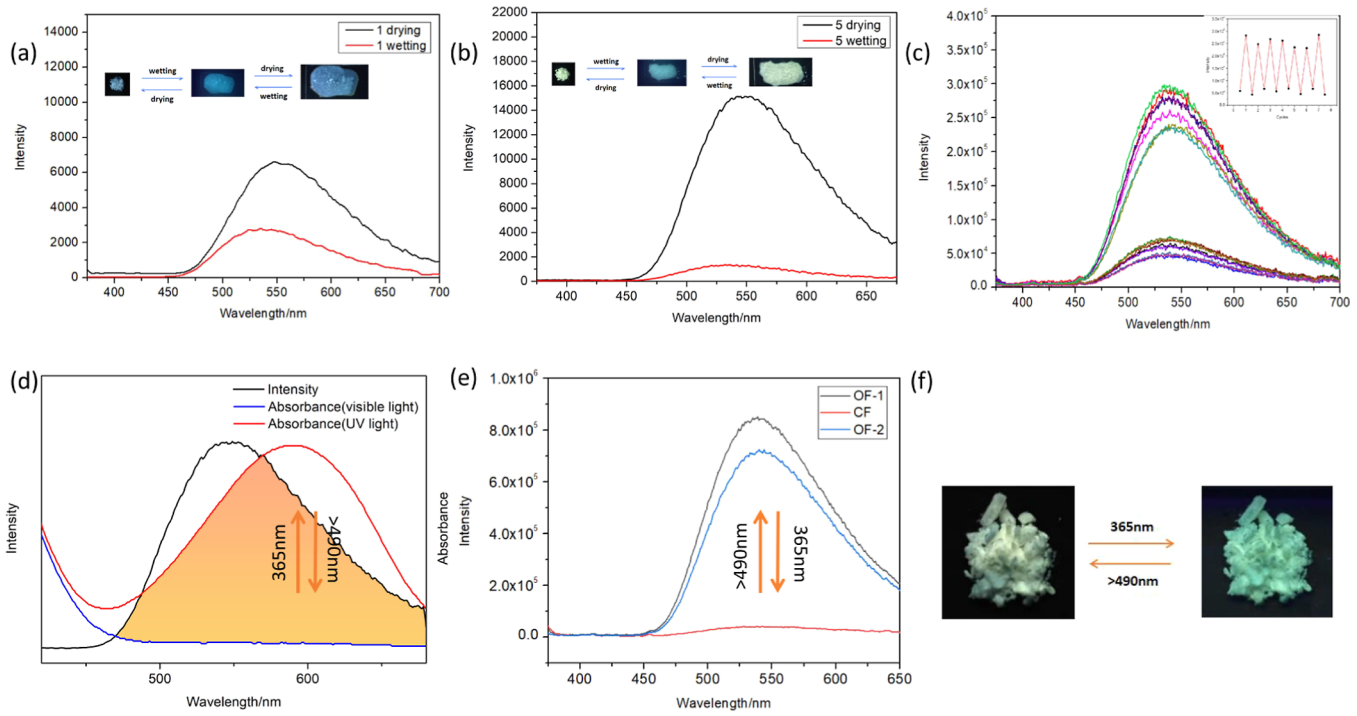

Figure 3. (a) Delayed luminescence spectra of xerogel **1** under drying/wetting conditions (λ_{ex} = 365 nm); inset: photographs of xerogel **1** before and after moistening and drying under 365 nm UV light. (b) Delayed luminescence spectra of xerogel **5** under drying/wetting conditions (λ_{ex} = 365 nm); inset: photographs of xerogel **5** before and after moistening and drying under 365 nm UV light. (c) Phosphorescence spectrum and (inset) intensity changes at 550 nm for gel **5** upon drying and 80% humidity (λ_{ex} = 365 nm). (d) Overlap of the absorption spectrum of DAE before and after 365 nm UV light and delayed photoluminescence emission spectrum of xerogel **5**. (e) Delayed photoluminescence emission spectra cycle of xerogel **5**/DAE under irradiation at 365 nm and over 490 nm. (f) Photographs of xerogel **5**/DAE with irradiation at 365 nm and over 490 nm under UV light.

Diarylethene and its derivatives are able to carry out triplet-to-singlet Förster resonance energy transfer (TS-FRET), possessing a marvelous light-responsive isomerization performance. Therefore, they are often used as photoresponsive switches in supramolecular systems.[47] According to the previous report, we synthesized a positively charged diarylethene derivative (DAE),[48] which was able to assemble with negatively charged CNSs in the gel system through electrostatic interaction. The excellent photoisomerization properties of the configured DAE solution can be seen from its UV spectra (Figure S26). The opened form DAE (OF-DAE) solution appeared as a yellow solution, but after being illuminated under 365 nm UV light, it turned into a closed form DAE (CF-DAE), which appeared as a blue solution. More interestingly, when CF-DAE was illuminated under visible light (>490 nm), it reverted back to OF-DAE, demonstrating the excellent reversible photoisomerization property of DAE. OF-DAE had no absorption at 450 nm −700 nm, nevertheless, under 365 nm UV illumination, the absorption peak continuously strengthened. The delayed photoluminescence spectra of xerogel **5** had a fairly good overlap with the absorption spectra of CF-DAE but could not overlap with the absorption spectra of OF-DAE (Figure 3d). Accordingly, it could be speculated that the triplet state energy of xerogel could be transferred into the singlet state of CF-DAE, thus prompting phosphorescence quenching in the gel system. Considering the excellent optical switching performance, DAE (2×10^{-5} M) was added into the gel system **5** and then lyophilized to obtain xerogel **5**/DAE. The delayed photoluminescence emission spectrum of the xerogel **5**/DAE showed a strong RTP emission at 546 nm (Figure 3e). When illuminated under 365 nm UV light, the RTP intensity significantly decreased, indicating that the RTP of the system was quenched. On the contrary, the RTP intensity of xerogel **5**/DAE recovered when exposed to visible light (>490 nm). The xerogel **5**/DAE showed yellow luminescence under 365 nm UV light. However, the RTP of this system was quenched after long-term UV illumination, showing green luminescence (Figure 3f). Finally, we verified the effect of xerogel sample thickness on the photoisomerization of DAE. As shown in Figure S27, the sample experiment with 0.2 and 0.5 mm thickness proved that the sample thickness had little influence on the photoisomerization of DAE and the photoresponse phosphorescence regulation of xerogel **5**/DAE. These results showed that DAE could be used as an excellent reversible light switch to control the multicolored luminescence of gel system.

Based on the fact that the RTP intensity of xerogel depended on the water content and the light absorption of DAE, the gel system exhibited good multiswitch regulation characteristics. First, the xerogel **5**/DAE was kept on the glass, and a blue light-emitting hydrogel was obtained. After drying, xerogel **5**/DAE showed a light-yellow emission under UV light. Intriguingly, xerogel **5**/DAE showed a bluish-green light after long-term irradiation with 365 nm UV light. We could infer that when water was used to write on the xerogel, the luminescent xerogel RTP was quenched, leaving only blue fluorescence. According to the above behavior, characters "NK" were written on the surface of xerogel. Under 365 nm UV light, the blue fluorescence of the characters "NK" on the xerogel **5**/DAE could be distinctly discerned (Figure 4a).

https://doi.org/10.1021/acsami.3c17214
ACS Appl. Mater. Interfaces 2024, 16, 5149−5157

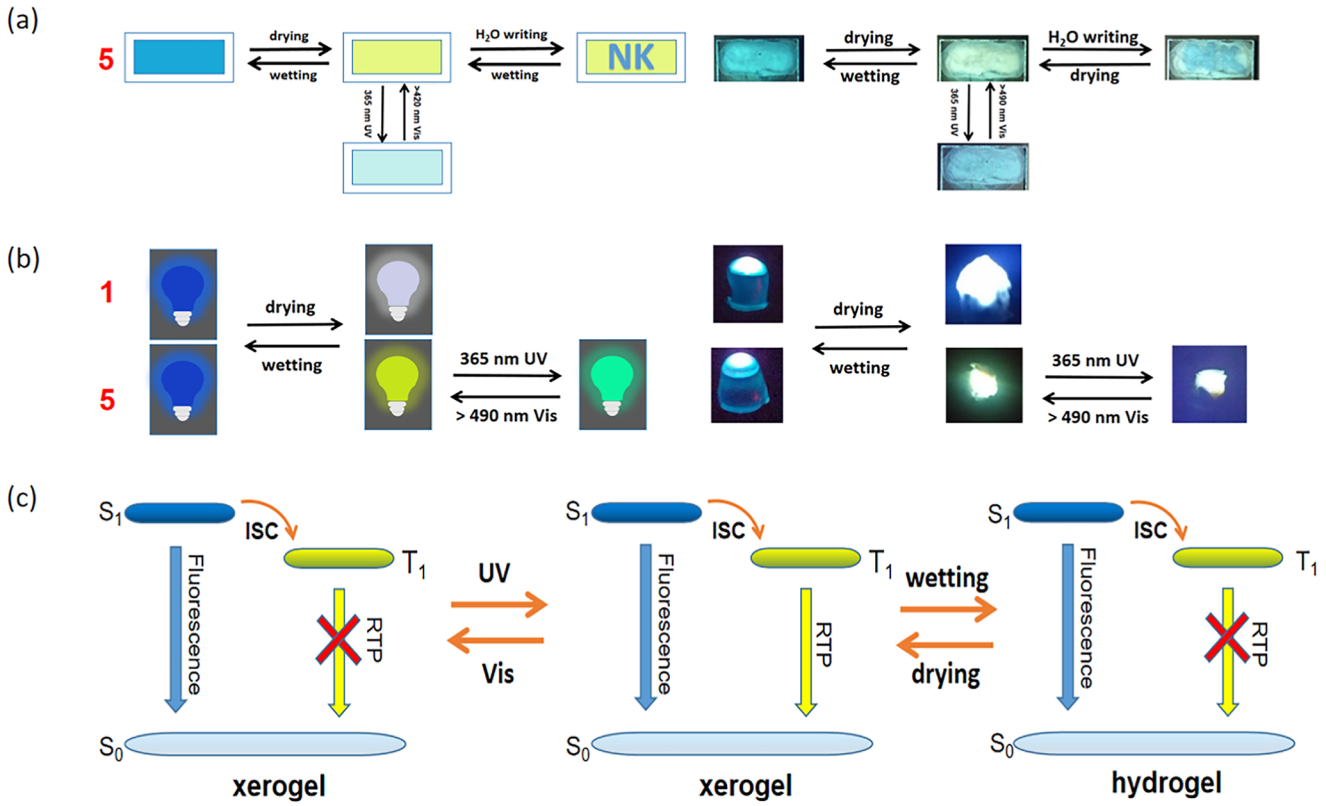

Figure 4. (a) Photographs of gel **5**/DAE dropped onto the glass and characters depicted by water before and after drying under UV light. (b) Photographs of light-emitting diodes (xerogel is fixed on the diode surface with poly(methyl methacrylate); λ_{ex} = 365 nm). (c) Schematic illustration of the reversible wetting−drying regulation and the reversible light-regulated TS-FRET processes.

Relatively, the blue fluorescence of "NK" on xerogel **1** was blurred due to the weak RTP intensity (Figure S28). Subsequently, the gel system was coated on the upper surfaces of the 365 nm light-emitting diodes to form the light-emitting diode gel system (Figure 4b). When the diodes were powered, hydrogel **1** and hydrogel **5** both emitted bright blue light. Diodes coated with xerogel **1** and xerogel **5**/DAE showed different changes in light emission behaviors. The diode coated with xerogel **1** exhibited blue-white light emission, while the diode coated with xerogel **5** exhibited yellow light. After long-term irradiation with 365 nm UV light, the diode coated with xerogel **5** turned white-green with light emission.

The possible mechanism of drying−wetting switch regulation is shown in Figure 4c: **G** was able to promote effective ISC from S_1 to T_1 through the spin−orbit coupling, thereby leading to phosphorescence emission. The rigid hydrogen-bonding network structure and the host−guest interactions in the xerogel could inhibit the ISC, which enhanced the RTP from T_1 to S_0, showing fluorescence−phosphorescence dual emission performance. On the contrary, the quenching effect of water promoted the nonradiative transition and eventually led to phosphorescence quenching, so only strong blue fluorescence could be attained. On the other hand, the reversible configuration transformation of DAE could be applied as an excellent reversible light regulation switch. OF-DAE could not affect the luminescence of the system. However, the absorption of CF-DAE and the phosphorescence emission of xerogel overlapped pretty well; thus, the RTP of xerogel could be suppressed through the triplet state to singlet TS-FRET, achieving phosphorescence quenching. Therefore, this kind of reversible luminescent gel material with multi-response characteristics may have potential applications in information storage, printing inks, water sensors, and orientation materials.

CONCLUSIONS

In summary, we synthesized a PEG−PPG-PEG block polymer **G** with brominated aromatic aldehydes as the core, which threaded ECDs to form polypseudorotaxane. Polypseudorotaxane can assemble with negatively charged CNSs through electrostatic interactions, forming a hydrogel in aqueous solution. The hydrogel had a blue fluorescence emission, and the lyophilized xerogel has a rigid network structure, which restricted vibration relaxation, showing a fluorescence−phosphorescence dual emission. Moreover, when ECDs were continuously added to the gel system, the phosphorescence emission intensity of the supramolecular xerogel would increase. The gel system was humidity responsive, and the change of the phosphorescence behavior could be adjusted by dry/wet conditions. Interestingly, as a reversible light switch, the DAE could regulate the RTP characteristics of supramolecular systems. This multistimulus-responsive luminescent supramolecular gel system may provide a new idea for the construction of tunable multicolor RTP materials.

EXPERIMENTAL SECTION

Materials. All reagents and solvents were commercially available and used without further purification unless otherwise noted. The core chemical CNS was purchased from BYK-Chemie GmbH. ECD was purchased from Zhiyuan Biotechnology. Compounds of DAE[48] were prepared by literature methods or modified literature methods.

https://doi.org/10.1021/acsami.3c17214
ACS Appl. Mater. Interfaces 2024, 16, 5149−5157

Procedure for the Synthesis of P-OTs. Poly(ethylene glycol)-*block*-poly(propylene glycol)-*block*-poly(ethylene glycol) (5.5 g, 5 mmol, the average molecular weight is 1100, PEG/PPG = 1:9) and triethylamine (1.05 mL, 7.5 mmol) were dissolved in 100 mL of anhydrous CH_2Cl_2 under a N_2 atmosphere. Then, 4-methylbenzenesulfonyl chloride (0.9533 g, 5 mmol) was slowly dropped into the solution under the ice bath condition. The mixture was stirred for 18 h at room temperature. Evaporation of the solvent under reduced pressure and purification by column chromatography using CH_2Cl_2/CH_3OH (40:1, V/V) as the eluent afforded 3.37 g of P-OTs in 53.7% yield.

Procedure for the Synthesis of G. 4-Bromo-2,5-dihydroxybenzaldehyde (100 mg, 0.46 mmol), P-OTs (1.34 g, 1.07 mmol, the average molecular weight is 1250), and anhydrous potassium carbonate (600 mg, 4.35 mmol) in CH_3CN (30 mL) were stirred for 24 h at 80 °C. After cooling to room temperature, the reaction mixture was poured into water, extracted with CH_2Cl_2, and dried with Na_2SO_4. Evaporation of the solvent under reduced pressure and purification by column chromatography using CH_2Cl_2/CH_3OH (20:1, V/V) as an eluent afforded 0.57 g of **G** in 52.3% yield.

■ ASSOCIATED CONTENT

Supporting Information

The Supporting Information is available free of charge at https://pubs.acs.org/doi/10.1021/acsami.3c17214.

Additional experimental details and methods; synthetic route of P-OTs, **G**, and DAE; NMR and MS data; preparation of the gel system; 2D ROESY spectra of pseudorotaxane; SEM images of xerogel systems; UV/vis spectra, photoluminescence spectrum, and phosphorescence spectrum; lifetime decay curves and photoluminescence quantum yield graphs; luminescence photographs of gel systems; and CIE chromaticity diagram data (PDF)

■ AUTHOR INFORMATION

Corresponding Authors

Yong Chen − *College of Chemistry, State Key Laboratory of Elemento-Organic Chemistry, Nankai University, Tianjin 300071, P. R. China*; Email: chenyong@nankai.edu.cn

Yu Liu − *College of Chemistry, State Key Laboratory of Elemento-Organic Chemistry, Nankai University, Tianjin 300071, P. R. China*; orcid.org/0000-0001-8723-1896; Email: yuliu@nankai.edu.cn

Authors

Songen Liu − *College of Chemistry, State Key Laboratory of Elemento-Organic Chemistry, Nankai University, Tianjin 300071, P. R. China*

Yi Zhang − *College of Chemistry, State Key Laboratory of Elemento-Organic Chemistry, Nankai University, Tianjin 300071, P. R. China*

Jianqiu Li − *College of Chemistry, State Key Laboratory of Elemento-Organic Chemistry, Nankai University, Tianjin 300071, P. R. China*

Conghui Wang − *College of Chemistry, State Key Laboratory of Elemento-Organic Chemistry, Nankai University, Tianjin 300071, P. R. China*

Complete contact information is available at: https://pubs.acs.org/10.1021/acsami.3c17214

Author Contributions

S.L., Y.Z., J.L., and H.W. synthesized the compounds and performed experiments. S.L collected data and summarized and wrote the manuscript. This project was edited and supervised by C.Y. and Y.L. All authors have given approval to the final version of the manuscript.

Notes

The authors declare no competing financial interest.

■ ACKNOWLEDGMENTS

This work was financially supported by the National Natural Science Foundation of China (grant nos. 22131008 and 21971127). We thank the Fundamental Research Funds for the Central Universities and the Haihe Laboratory of Sustainable Chemical Transformations for financial support.

■ REFERENCES

(1) Zhang, Y.; Sun, Q.; Yue, L.; Wang, Y.; Cui, S.; Zhang, H.; Xue, S.; Yang, W. Room Temperature Phosphorescent (RTP) Thermoplastic Elastomers with Dual and Variable RTP Emission, Photo-Patterning Memory Effect, and Dynamic Deformation RTP Response. *Adv. Sci.* **2022**, *9*, 2103402.

(2) Guo, J.; Yang, C.; Zhao, Y. Long-Lived Organic Room-Temperature Phosphorescence from Amorphous Polymer Systems. *Acc. Chem. Res.* **2022**, *55*, 1160−1170.

(3) Zhou, B.; Yan, D. Long Persistent Luminescence from Metal-Organic Compounds: State of the Art. *Adv. Funct. Mater.* **2023**, *33*, 2300735.

(4) Garain, S.; Garain, B. C.; Eswaramoorthy, M.; Pati, S. K.; George, S. J. Light-Harvesting Supramolecular Phosphors: Highly Efficient Room Temperature Phosphorescence in Solution and Hydrogels. *Angew. Chem., Int. Ed.* **2021**, *60*, 19720−19724.

(5) Wang, C.; Ma, X. K.; Guo, P.; Jiang, C.; Liu, Y. H.; Liu, G.; Xu, X.; Liu, Y. Highly Reversible Supramolecular Light Switch for NIR Phosphorescence Resonance Energy Transfer. *Adv. Sci.* **2022**, *9*, 2103041.

(6) Wei, P.; Zhang, X.; Liu, J.; Shan, G. G.; Zhang, H.; Qi, J.; Zhao, W.; Sung, H. H. Y.; Williams, I. D.; Lam, J. W. Y.; Tang, B. Z. New Wine in Old Bottles: Prolonging Room-Temperature Phosphorescence of Crown Ethers by Supramolecular Interactions. *Angew. Chem., Int. Ed.* **2020**, *59*, 9293−9298.

(7) Zhang, Z. Y.; Xu, W. W.; Xu, W. S.; Niu, J.; Sun, X. H.; Liu, Y. A Synergistic Enhancement Strategy for Realizing Ultralong and Efficient Room-Temperature Phosphorescence. *Angew. Chem., Int. Ed.* **2020**, *59*, 18748−18754.

(8) Wang, H. J.; Xing, W. W.; Yu, Z. H.; Zhang, H. Y.; Xu, W. W.; Liu, Y. Noncovalent Bridged Bis(Coumarin-24-Crown-8) Phosphorescent Supramolecular Switch. *Adv. Opt. Mater.* **2022**, *10*, 2201903.

(9) Dai, X. Y.; Hu, Y. Y.; Sun, Y.; Huo, M.; Dong, X.; Liu, Y. A Highly Efficient Phosphorescence/Fluorescence Supramolecular Switch Based on a Bromoisoquinoline Cascaded Assembly in Aqueous Solution. *Adv. Sci.* **2022**, *9*, 2200524.

(10) Shen, F. F.; Chen, Y.; Dai, X. Y.; Zhang, H. Y.; Zhang, B.; Liu, Y. H.; Liu, Y. Purely organic light-harvesting phosphorescence energy transfer by β-cyclodextrin pseudorotaxane for mitochondria targeted imaging. *Chem. Sci.* **2021**, *12*, 1851−1857.

(11) Sun, X. R.; Yang, H. P.; Zhang, W.; Zhang, S.; Hu, J. H.; Liu, M.; Zeng, X.; Li, Q.; Redshaw, C.; Tao, Z.; Xiao, X. Supramolecular Room-Temperature Phosphorescent Hydrogel Based on Hexamethyl Cucurbit[5]uril for Cell Imaging. *ACS Appl. Mater. Interfaces* **2023**, *15*, 4668−4676.

(12) Ma, Y. J.; Xiao, G.; Fang, X.; Chen, T.; Yan, D. Leveraging Crystalline and Amorphous States of a Metal-Organic Complex for Transformation of the Photosalient Effect and Positive-Negative Photochromism. *Angew. Chem., Int. Ed.* **2023**, *62*, No. e202217054.

(13) Zhou, B.; Qi, Z.; Dai, M.; Xing, C.; Yan, D. Ultralow-loss Optical Waveguides through Balancing Deep-Blue TADF and Orange Room Temperature Phosphorescence in Hybrid Antimony Halide Microstructures. *Angew. Chem., Int. Ed.* **2023**, *62*, No. e202309913.

(14) Yang, D. D.; Meng, F.; Zheng, H. W.; Shi, Y. S. X.; Xiao, T.; Jin, B.; Liang, Q. F.; Zheng, X. J.; Tan, H. W. Two Multifunctional Stimuli-Responsive Materials with Room-Temperature Phosphorescence and Their Application in Multiple Dynamic Encryption. *Mater. Chem. Front.* **2022**, *6*, 2709−2717.
(15) Li, M.; Xie, W.; Cai, X.; Peng, X.; Liu, K.; Gu, Q.; Zhou, J.; Qiu, W.; Chen, Z.; Gan, Y.; Su, S. J. Molecular Engineering of Sulfur-Bridged Polycyclic Emitters Towards Tunable TADF and RTP Electroluminescence. *Angew. Chem. Int. Ed.* **2022**, *134*, No. e202209343.
(16) Xie, Z.; Zhang, X.; Wang, H.; Huang, C.; Sun, H.; Dong, M.; Ji, L.; An, Z.; Yu, T.; Huang, W. Wide-Range Lifetime-Tunable and Responsive Ultralong Organic Phosphorescent Multi-Host/Guest System. *Nat. Commun.* **2021**, *12*, 3522.
(17) Li, D.; Yang, Y.; Yang, J.; Fang, M.; Tang, B. Z.; Li, Z. Completely Aqueous Processable Stimulus Responsive Organic Room Temperature Phosphorescence Materials with Tunable Afterglow Color. *Nat. Commun.* **2022**, *13*, 347.
(18) Wang, C.; Qu, L.; Chen, X.; Zhou, Q.; Yang, Y.; Zheng, Y.; Zheng, X.; Gao, L.; Hao, J.; Zhu, L.; Pi, B.; Yang, C. Poly(arylene piperidine) Quaternary Ammonium Salts Promoting Stable Long-Lived Room-Temperature Phosphorescence in Aqueous Environment. *Adv. Mater.* **2022**, *34*, 2204415.
(19) Li, D.; Yang, J.; Fang, M. M.; Tang, B. Z.; Li, Z. Stimulus-Responsive Room Temperature Phosphorescence Materials with Full-Color Tunability from Pure Organic Amorphous Polymers. *Sci. Adv.* **2022**, *8*, No. eabl8392.
(20) Tao, W.; Zhou, Y.; Lin, F.; Gao, H.; Chi, Z.; Liang, G. Strain-Responsive Persistent Room-Temperature Phosphorescence from Halogen-Free Polymers for Early Damage Reporting through Phosphorescence Lifetime and Image Analysis. *Adv. Opt. Mater.* **2022**, *10*, 2102449.
(21) Dai, W.; Niu, X.; Wu, X.; Ren, Y.; Zhang, Y.; Li, G.; Su, H.; Lei, Y.; Xiao, J.; Shi, J.; Tong, B.; Cai, Z.; Dong, Y. Halogen Bonding: A New Platform for Achieving Multi-Stimuli-Responsive Persistent Phosphorescence. *Angew. Chem., Int. Ed.* **2022**, *61*, No. e202200236.
(22) Wu, H.; Zhao, P.; Li, X.; Chen, W.; Agren, H.; Zhang, Q.; Zhu, L. Tuning for Visible Fluorescence and Near-Infrared Phosphorescence on a Unimolecular Mechanically Sensitive Platform via Adjustable CH-π Interaction. *ACS Appl. Mater. Interfaces* **2017**, *9*, 3865−3872.
(23) Yang, Y.; Wang, K. Z.; Yan, D. Ultralong Persistent Room Temperature Phosphorescence of Metal Coordination Polymers Exhibiting Reversible pH-Responsive Emission. *ACS Appl. Mater. Interfaces* **2016**, *8*, 15489−15496.
(24) Chen, J.; Lin, F.; Liang, G.; Huang, H.; Qin, T.; Yang, Z.; Chi, Z. Asymmetric Diarylamine Guests for a Host-Guest System with Stimulus-Responsive Room Temperature Phosphorescence. *J. Mater. Chem. C* **2023**, *11*, 6290−6295.
(25) Wang, C.; Chen, Y.; Xu, Y.; Ran, G.; He, Y.; Song, Q. Aggregation-Induced Room-Temperature Phosphorescence Obtained from Water-Dispersible Carbon Dot-Based Composite Materials. *ACS Appl. Mater. Interfaces* **2020**, *12*, 10791−10800.
(26) Yang, J.; Song, J. I.; Song, Q.; Rho, J. Y.; Mansfield, E. D. H.; Hall, S. C. L.; Sambrook, M.; Huang, F.; Perrier, S. Hierarchical Self-Assembled Photo-Responsive Tubisomes from a Cyclic Peptide-Bridged Amphiphilic Block Copolymer. *Angew. Chem., Int. Ed.* **2020**, *59*, 8860−8863.
(27) Chen, X. M.; Feng, W. J.; Bisoyi, H. K.; Zhang, S.; Chen, X.; Yang, H.; Li, Q. Light-Activated Photodeformable Supramolecular Dissipative Self-Assemblies. *Nat. Commun.* **2022**, *13*, 3216.
(28) Su, T.; Liu, Y. H.; Chen, Y.; Liu, Y. A Tunable Phosphorescence Supramolecular Switch by an Anthracene Photoreaction in Aqueous Solution. *J. Mater. Chem. C* **2022**, *10*, 2623−2630.
(29) Xing, C.; Zhou, B.; Yan, D.; Fang, W. H. Dynamic Photoresponsive Ultralong Phosphorescence from One-Dimensional Halide Microrods Toward Multilevel Information Storage. *CCS Chem.* **2023**, *5*, 2866−2876.
(30) Zheng, Y.; Zhou, Q.; Yang, Y.; Chen, X.; Wang, C.; Zheng, X.; Gao, L.; Yang, C. Full-Color Long-Lived Room Temperature Phosphorescence in Aqueous Environment. *Small* **2022**, *18*, 2201223.
(31) Dai, D. H.; Li, Z.; Yang, J.; Wang, C. Y.; Wu, J. R.; Wang, Y.; Zhang, D. M.; Yang, Y. W. Supramolecular Assembly-Induced Emission Enhancement for Efficient Mercury(II) Detection and Removal. *J. Am. Chem. Soc.* **2019**, *141*, 4756−4763.
(32) Liu, Z.; Li, D.; Tong, L.; Meng, Y.; Fang, M.; Yang, J.; Tang, B. Z.; Li, Z. The Simpler, the Better: Organic Materials with Adsorption-Induced Room-Temperature Phosphorescence for Anti-Counterfeiting and Dyeing Applications. *Adv. Opt. Mater.* **2023**, *11*, 2203069.
(33) Liu, F.; Li, Z.; Li, Y.; Feng, Y.; Feng, W. Room-Temperature Phosphorescent Fluorine-Nitrogen Co-Doped Carbon Dots: Information Encryption and Anti-Counterfeiting. *Carbon* **2021**, *181*, 9−15.
(34) Zhou, H. Y.; Zhang, D. W.; Li, M.; Chen, C. F. A Calix[3]acridan-Based Host-Guest Cocrystal Exhibiting Efficient Thermally Activated Delayed Fluorescence. *Angew. Chem., Int. Ed.* **2022**, *61*, No. e202117872.
(35) Corsini, F.; Nitti, A.; Tatsi, E.; Mattioli, G.; Botta, C.; Pasini, D.; Griffini, G. Large-Area Semi-Transparent Luminescent Solar Concentrators Based on Large Stokes Shift Aggregation-Induced Fluorinated Emitters Obtained Through a Sustainable Synthetic Approach. *Adv. Opt. Mater.* **2021**, *9*, 2100182.
(36) Yu, M. L.; Zhao, W. L.; Ni, F.; Zhao, Q.; Yang, C. L. Photoswitchable Thermally Activated Delayed Fluorescence Nanoparticles for "Double-Check" Confocal and Time-Resolved Luminescence Bioimaging. *Adv. Opt. Mater.* **2022**, *10*, 2102437.
(37) Li, D.; Lu, F.; Wang, J.; Hu, W.; Cao, X. M.; Ma, X.; Tian, H. Amorphous Metal-Free Room-Temperature Phosphorescent Small Molecules with Multicolor Photoluminescence via a Host-Guest and Dual-Emission Strategy. *J. Am. Chem. Soc.* **2018**, *140*, 1916−1923.
(38) Neisi, E.; Tehrani, A. D.; Shamlouei, H. R. Fully bio-based supramolecular gel based on cellulose nanowhisker gallate by cyclodextrin host-guest chemistry. *Carbohydr. Polym.* **2023**, *299*, 120222.
(39) Wang, H.; Zhu, C. N.; Zeng, H.; Ji, X.; Xie, T.; Yan, X.; Wu, Z. L.; Huang, F. Reversible Ion-Conducting Switch in a Novel Single-Ion Supramolecular Hydrogel Enabled by Photoresponsive Host-Guest Molecular Recognition. *Adv. Mater.* **2019**, *31*, 1807328.
(40) Wang, J.; Huang, Z.; Ma, X.; Tian, H. Visible-Light-Excited Room-Temperature Phosphorescence in Water by Cucurbit[8]uril-Mediated Supramolecular Assembly. *Angew. Chem., Int. Ed.* **2020**, *59*, 9928−9933.
(41) Ohshita, N.; Motoyama, K.; Iohara, D.; Hirayama, F.; Taharabaru, T.; Watabe, N.; Kawabata, Y.; Onodera, R.; Higashi, T. Polypseudorotaxane-Based Supramolecular Hydrogels Consisting of Cyclodextrins and Pluronics as Stabilizing Agents for Antibody Drugs. *Carbohydr. Polym.* **2021**, *256*, 117419.
(42) Rong, Y.; Liu, R.; Jin, P.; Liu, C.; Wang, X.; Fang, L.; Chen, L.; Wu, W.; Yang, C. Photoprinting and Expansion-Induced Erasure with Supramolecular Hydrogels Crosslinked by Pseudorotaxanation. *J. Mater. Chem. A* **2023**, *11*, 5895−5901.
(43) Zhang, Y.; Zhang, C.; Chen, Y.; Yu, J.; Chen, L.; Zhang, H.; Xu, X.; Liu, Y. Photo-Controlled Reversible Multicolor Room-Temperature Phosphorescent Solid Supramolecular Pseudopolyrotaxane. *Adv. Opt. Mater.* **2022**, *10*, 2102169.
(44) Li, J. J.; Zhang, H. Y.; Zhang, Y.; Zhou, W. L.; Liu, Y. Room-Temperature Phosphorescence and Reversible White Light Switch Based on a Cyclodextrin Polypseudorotaxane Xerogel. *Adv. Opt. Mater.* **2019**, *7*, 1900589.
(45) Zhang, Y.; Liang, L.; Chen, Y.; Chen, X. M.; Liu, Y. Construction and Efficient Dye Adsorption of Supramolecular Hydrogels by Cyclodextrin Pseudorotaxane and Clay. *Soft Matter* **2019**, *15*, 73−77.
(46) Li, D.; Liu, Z.; Fang, M.; Yang, J.; Tang, B. Z.; Li, Z. Ultralong Room-Temperature Phosphorescence with Second-level Lifetime in Water Based on Cyclodextrin Supramolecular Assembly. *ACS Nano* **2023**, *17*, 12895−12902.

https://doi.org/10.1021/acsami.3c17214
ACS Appl. Mater. Interfaces 2024, 16, 5149−5157

(47) Wu, H.; Chen, Y.; Dai, X. Y.; Li, P. Y.; Stoddart, J. F.; Liu, Y. In Situ Photoconversion of Multicolor Luminescence and Pure White Light Emission Based on Carbon Dot-Supported Supramolecular Assembly. *J. Am. Chem. Soc.* **2019**, *141*, 6583−6591.
(48) Liu, G.; Zhang, Y. M.; Wang, C.; Liu, Y. Dual Visible Light-Triggered Photoswitch of a Diarylethene Supramolecular Assembly with Cucurbit[8]uril. *Chem.—Eur. J.* **2017**, *23*, 14425−14429.

https://doi.org/10.1021/acsami.3c17214
ACS Appl. Mater. Interfaces 2024, 16, 5149−5157